CEAS Space Journal (2024) 16:87–95
https://doi.org/10.1007/s12567-023-00491-2

ORIGINAL PAPER

Investigation of X-band and Ka-band amplitude scintillation based on measurement data collected during ESA's BepiColombo superior solar conjunction campaign

Shun-Ping Chen[1] · **Marco Lanucara**[2] · **Jose Villalvilla**[2]

Received: 25 October 2022 / Revised: 2 February 2023 / Accepted: 14 March 2023 / Published online: 31 March 2023

Abstract
Solar phase scintillation and solar amplitude scintillation are fundamentally important in deep space mission operations for designing a communication system capable of transmitting signals when the signal path is close to the Sun. The ESA's BepiColombo measurement data were analyzed in a previous paper in terms of the power spectral density of the solar phase scintillation, also with a comparison with Woo's solar phase scintillation theory, when X-band and Ka-band signals propagate close to the Sun with a small Sun-Earth-Probe (SEP) angle during the superior solar conjunction campaign in March 2021 in its cruise phase to Mercury. In this paper the solar amplitude scintillation is analyzed both by calculating the power spectral density and the scintillation index. The results of scintillation index, derived from these measurement data, fit the NASA JPL's scintillation index model.

Keywords Deep space communications · Solar wind · Solar plasma · Phase scintillation · Amplitude scintillation · Intensity scintillation · Scattering · Solar superior conjunction · SEP Sun-Earth-probe angle · BepiColombo · ESA European Space Agency · NASA National Aeronautics and Space Administration · JPL Jet propulsion laboratory

1 Previous projects and the novel investigation results

Deep space communication technologies have been developed continuously in the last decades, both in the radio frequency bands and in the infrared spectrum for laser optical communications. Due to the solar wind activities and the ionized solar plasma, a radio transmission suffers phase and amplitude scintillation, as well as spectral broadening for radio paths close to the Sun with a heliocentric distance of 2 R_s - 215 R_s where R_s is the Sun radius. The spectral broadening effect and the intensity of the solar scintillation depend on the solar-wind velocity and electron-density irregularities, and were investigated and described in detail in [1–7].

✉ Shun-Ping Chen
shun-ping.chen@h-da.de

[1] Institute of Communication Technologies, Darmstadt University of Applied Sciences, Birkenweg 8, DE-64295 Darmstadt, Germany

[2] ESA/ESOC European Space Agency, Operations Centre, Robert-Bosch-Straße 5, DE-64293 Darmstadt, Germany

The scintillation index and the scintillation spectral density distribution have proven to be very useful methods to characterize radio scattering measurement results. The better understanding of the solar plasma effects on the scattering of radio waves is essential for communications' design and spacecraft's navigation in interplanetary missions for small SEP angles.

In a previous paper [8] the phase scintillations' dependence on SEP angles was investigated and the results were compared with ESA's BepiColombo measurement data [9], when operating in coherent transponder mode, generally for X-band and Ka-band near the Sun.

The amplitude scintillation effects with small SEP angles were investigated in the past and a model was described by JPL (Jet Propulsion Laboratories) at California Institute of Technology in cooperation with NASA (NASA National Aeronautics and Space Administration) [1, 5, 6, 10, 11], and was validated by investigating ESA's solar scintillation measurement data [12]. In [6, 11] the measurement data and scintillation indices of different NASA missions like Viking (1976 Ingress and Egress), Ulysses (1991 Ingress and Egress), Mars Global Surveyor (1998), Cassini (2000), Deep Space 1 (2000), Stardust (2000) and Cassini (2001)

were compared with the model. Despite small deviation of the measurement results from the model, the general trends of the scintillation indices match pretty well with the model. This confirms that the JPL DSMS scintillation model can be used for amplitude scintillation investigations. It should be noted that the assumed solar wind electron density distribution in the model is an average value which could change not only depending on the SEP angles, but also depending on the solar corona activities which can be considered by three different reference factors 1, 1.5 or 2.41 respectively [12].

As proposed in [6], the models should be continuously compared with the new mission measurement data and refined as a function of solar elongation angle and perhaps as a function of other parameters such as solar cycle phase and sub-solar latitude. Encouraged by such proposals, in this paper the solar amplitude scintillation, in terms of scintillation index in the time domain, after bandpass filter postprocessing of ESA's BepiColombo measurement data collected during the solar superior conjunction, was investigated and compared with the NASA JPL DSMS model. Furthermore, the power spectral density distributions were calculated which show more clearly and in detail the different spectral characteristics depending on SEP angles.

To summarize the novelties of the results in this paper:

a) Most publications about the solar amplitude scintillation or intensity scintillation up to now use the scintillation index as the main characteristic parameter to describe the amplitude scintillation effect. This is also done in this paper with a new set of BepiColombo measurement data;

b) Few publications in the past decades deal directly with the spectral density analysis of the measurement data in context with amplitude scintillation. In this paper also the power spectral density is analyzed based on the BepiColombo measurement data in the superior solar conjunction phase. In section 5, it can be clearly recognized, that the results of the power spectral analysis show more precisely the variable details or the changed slopes between 0.1 Hz–100 Hz directly depending on SEP angles, which could not be perceived by the scintillation index directly;

c) Due to the paucity of the Ka-band measurements, more mission measurement data especially in Ka-band should be taken into consideration and additional measurements should be acquired to supplement this data set to better characterize solar scintillation effects at Ka-band [6]. Therefore the valuable ESA's BepiColombo measurement data definitely contribute to this field;

d) The calculated scintillation indices in X-band and Ka-band, based on the BepiColombo measurement data, confirm the NASA JPL model [4];

e) The changed slopes differently to the Kolmogorow turbulence theory between 0.1 and 100 Hz mentioned in point (b) depend not only on the electron density irregularities, but also on the effects during transient events, or during signal transit through coronal holes, or depending on the solar cycle phase, or sub-solar latitude, as discussed in [6]. Therefore the precise power spectral density analysis of the amplitude scintillation can possibly be used to explain the dominating effects in the spectral range of 0.1–100 Hz, directly indicating the solar corona activities.

2 Theoretical background about amplitude scintillation

The solar amplitude scintillation was investigated in the past [10–12]. The measured intensity generally consists of solar intensity scintillation and additive Gaussian white noise [12]. The impact of the additive Gaussian white noise becomes very critical, when the open loop receiver in the ground station converts the X-band and Ka-band signal to the baseband. The raw measurement data [9] in baseband were unfiltered. In this case, the thermal noise within and outside the signal band will disturb the solar scintillation estimation significantly, sometimes even overdominate the solar scintillation to make it impossible to receive the pure solar amplitude scintillation which is the focus of the research activity. To significantly reduce and remove the additive Gaussian thermal noise, the bandpass filtering with a bandwidth of ±100 Hz [12] will be necessary to remove the white noise outside the signal band.

The scintillation m' of combined signals, consisting of additive Gaussian white noise with total power P_N within the detection bandwidth, the signal power P_S and the scintillation m caused only by solar wind, can be written as [12]

$$m' = \frac{\sqrt{P_N^2 + 2 \cdot P_N \cdot P_S + P_S^2 \cdot m^2}}{P_N + P_S} \tag{1}$$

or

$$m' = \frac{\sqrt{1 + 2 \cdot SNR + SNR^2 \cdot m^2}}{1 + SNR}. \tag{2}$$

The following inverse relation can be used to derive the index m, which is the actual parameter of interest, from the index m' measured in a noisy context

$$m = \frac{\sqrt{m'^2 \cdot (1 + SNR)^2 - (1 + 2 \cdot SNR)}}{SNR} \tag{3}$$

as long as

$$m' > \frac{\sqrt{1 + 2 \cdot SNR}}{1 + SNR}. \tag{4}$$

If the condition (4) is not valid, then the pure solar amplitude scintillation index m can not be exactly derived from m'.

3 ESA's BepiColombo measurement data

In March 2021, during the cruise phase of ESA's BepiColombo mission to Mercury, valuable measurement data were collected during several days of the superior solar conjunction at SEP angles that varied from 1.2° to 5.1° at the slant range of 1.51 AU for the coherent X/X-band and X/Ka-band downlink. These data [9] are derived from the received spacecraft signals down-converted and sampled to obtain the complex waveform at baseband. The basic measurement parameters are listed in Table 1.

The data used for the present analysis were selected among the continuously collected measurement data during several campaign days, carefully avoiding data at low elevation or unstable weather conditions to avoid any potential impact of the troposphere contribution to the results, which in most of the cases, should be negligible compared to the contribution of solar plasma. The sampling rate for the measurement data is 2000 samples/sec. These amplitude data are first filtered and a total of 600,000 samples or 300 s are taken into account for the scintillation index calculation and the power spectral density (PSD) analysis which was performed by using the Matlab power spectral density algorithm based on the Burg method among many other different PSD estimation algorithms [13].

4 Filtered measurement data in X-band and Ka-band in time domain

In Fig. 1a–d, the time series of the intensities are displayed to show the fluctuations caused by the solar scintillation at SEP angle 5.1°, 3.6°, 2.9° and 1.2° for X-band measurements. In Fig. 2a–d, the time series of the intensities are displayed to show the fluctuations caused by the solar scintillation at SEP angle 5.1°, 3.6°, 2.9° and 1.2° for Ka-band measurements. It can be recognized clearly that the time series of the amplitude scintillation at 1.2° for both X-band and Ka-band during the 300 s of measurement data are significantly stronger than at SEP angle 5.1°, which can be explained by a reduction of the effect of solar plasma on the signal with a larger heliocentric distance, i.e. larger SEP angles.

Table 1 BepiColombo superior solar conjunction measurement parameters

Band	SEP [°]	Carrier Power Pc [dBm]	Th. Noise No [dBm/Hz]
X/X	5.1	−75.8	−120.6
X/X	3.6	−75.8	−120.8
X/X	2.9	−71.5	−120.4
X/X	1.2	−66.9	−118.2
X/Ka	5.1	−71.2	−117.2
X/Ka	3.6	−71.2	−117.1
X/Ka	2.9	−67.4	−114.6
X/Ka	1.2	−68.2	−116.8

The average values alone are not the proper parameter due to some configuration of modulation index and different carrier power levels P_c (see Table 1). Only the standard deviations together with the average values, the so-called scintillation index, determines the characteristics for the solar scintillation. In the titles of the figures, the abbreviations "si", "sp", "ap" correspond to the scintillation index, standard deviation and average values. Especially for X-band, it can be recognized clearly that the amplitude scintillation at SEP angle 1.2° is much stronger than at the SEP angle 5.1° due to the stronger influence of solar plasma on the signal.

5 Amplitude scintillation analysis of ESA's BepiColombo superior solar conjunction measurement data for X-band and Ka-band

The power spectral density of the amplitude scintillation is then estimated using the Burg's method, an autoregressive approach implemented by Matlab algorithm [13].

The above-mentioned time-domain amplitude data for X-band and Ka-band for different SEP angles are used for calculating amplitude scintillation power spectral densities. Figure 3a–d show the scintillation power spectral densities for X-band for the different SEP angles 5.1°, 3.6°, 2.9° and 1.2° calculated by the procedure described above. The amplitude scintillation spectral densities for SEP angles derived from the measurement data for Ka-band are shown in Fig. 4a–d for SEP = 5.1°, 3.6°, 2.9° and 1.2°.

It can be clearly seen, that beyond the spectral frequency of about 10–1000 Hz (100–1000 Hz for SEP 1.2°), a noise floor with a level of about -120 dBm/Hz prevails and overdominates over the X-band solar amplitude scintillation (see also Table 1).

It should be pointed out that Fig. 3, Fig. 4 present an increased X-band and Ka-band amplitude scintillation at frequencies above approximately 0.1 Hz, before the thermal noise floor becomes dominating at 10–1000 Hz (50 Hz - 1000 Hz for SEP 1.2°). This effect was also observed for solar phase scintillation [8].

The changed slopes between 0.1 Hz and 100 Hz depend not only on the electron density irregularities, but also on

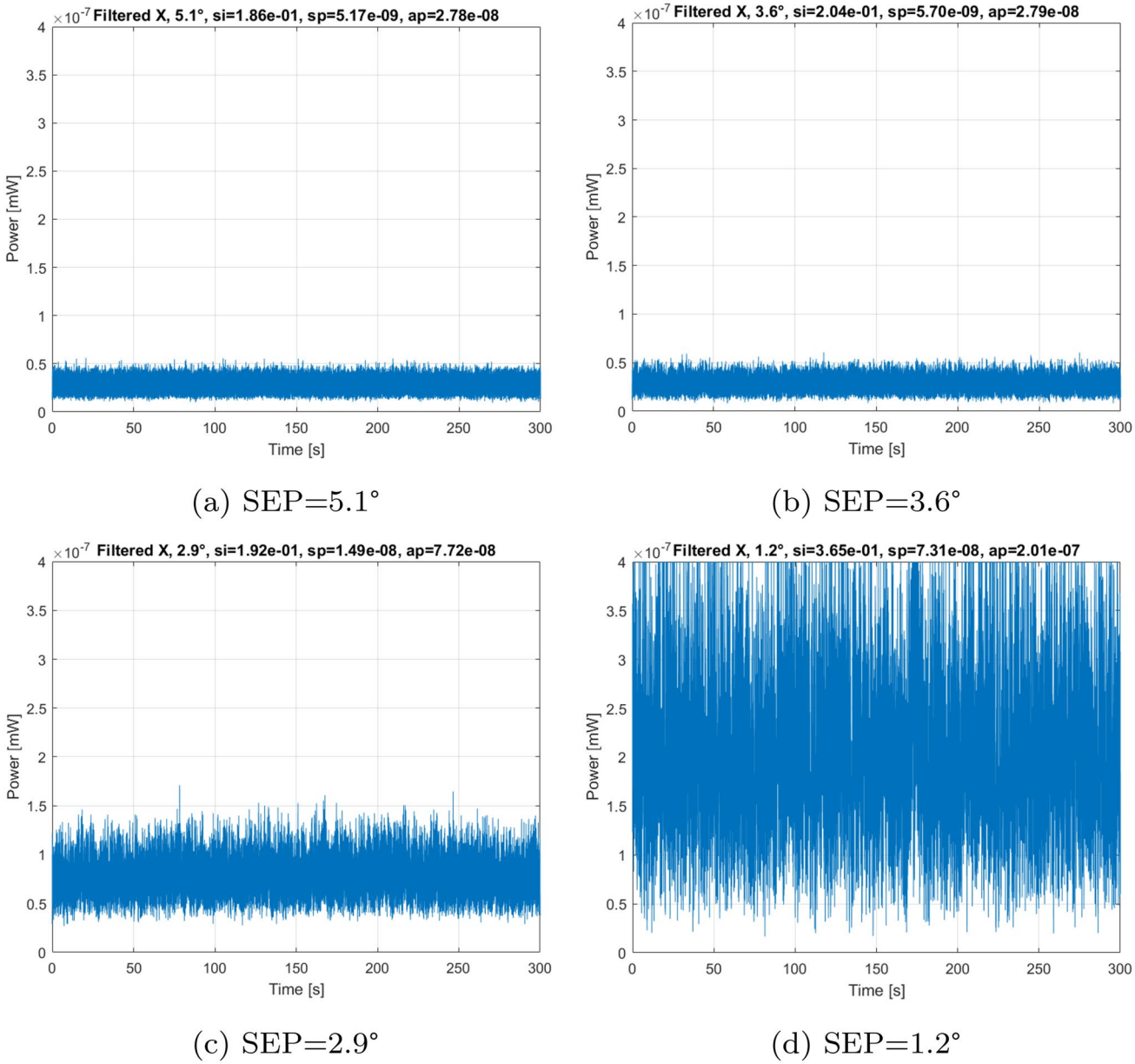

Fig. 1 Filtered X-band measurement data

the effects during transient events, or during signal transit through coronal holes, or depending even on the solar cycle phase and sub-solar latitude, as discussed in [5]. Therefore the precise power spectral density analysis of the amplitude scintillation can possibly show more details and can be used to explain the dominating effects in the spectral range of 0.1–100 Hz, directly indicating the solar corona activities.

6 Scintillation index derived from ESA's BepiColombo measurement data in comparison with NASA JPL DSMS model

Using the time-domain amplitude data, the signal to noise ratio (SNR), combined scintillation index m' and therefore also the solar scintillation index m can be derived.

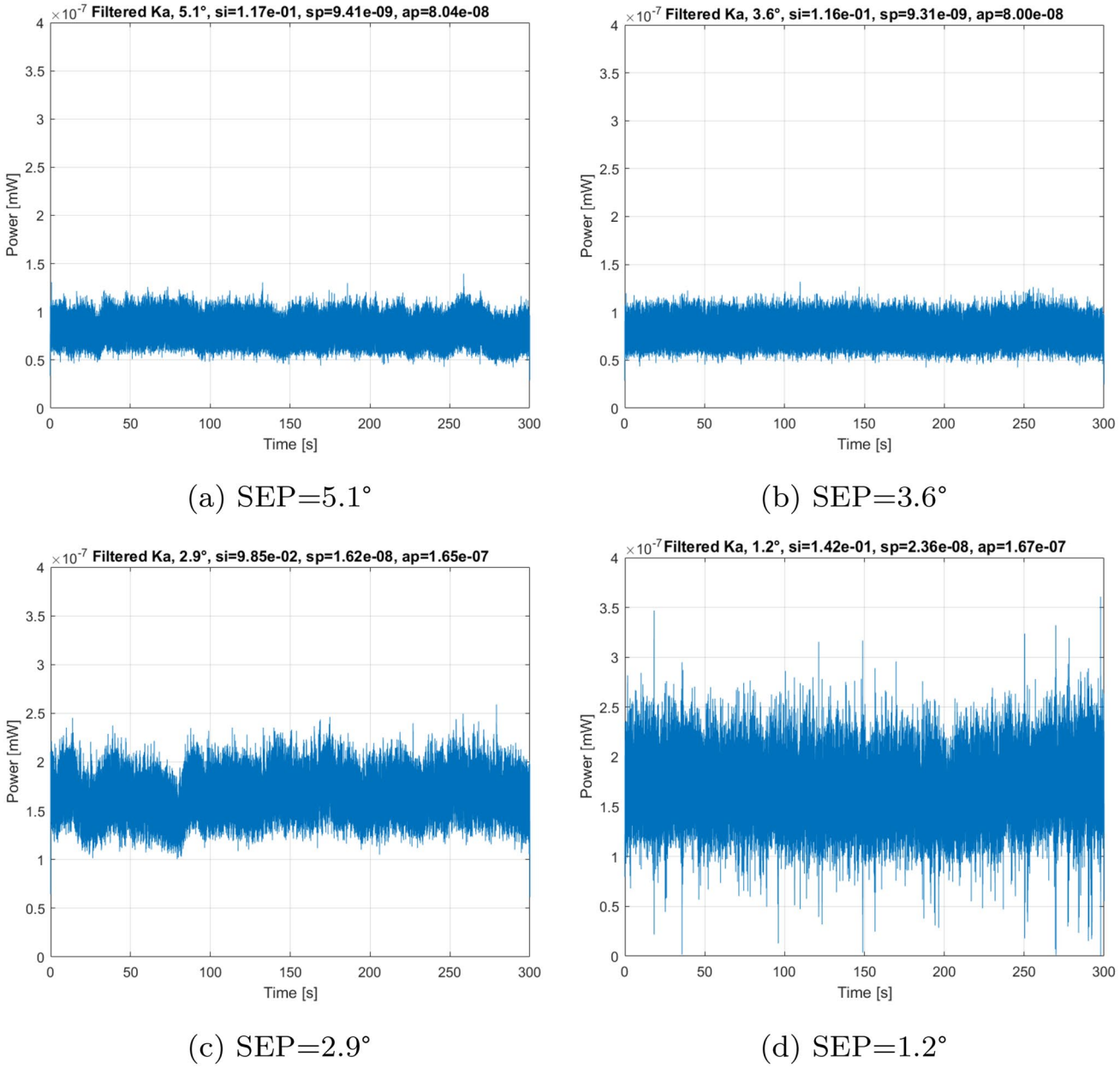

Fig. 2 Filtered Ka-band measurement data

For Ka-band measurement data, the condition equation (4) is not valid for SEP 3.6° and SEP 2.9°, therefore m (only caused by solar wind scintillation) can not be derived from m', i.e. the effect of additive Gaussian white noise can not be removed and the pure solar wind scintillation can not be separated, therefore the higher combined scintillation index m' is displayed in Fig. 6.

The simplified solar scintillation model proposed by JPL in [4] and the scintillation index calculations based on the BepiColombo measurement data are drawn in Fig. 5 for X-band and Fig. 6 for Ka-band. Generally the scintillation indices derived by ESA's BepiColombo measurement data coincide pretty well with the JPL DSMS model, which confirms the JPL scintillation index model.

7 Conclusions

ESA's BepiColombo open loop baseband measurement data collected during the superior solar conjunction campaign in March 2021 have been used to calculate the power spectral

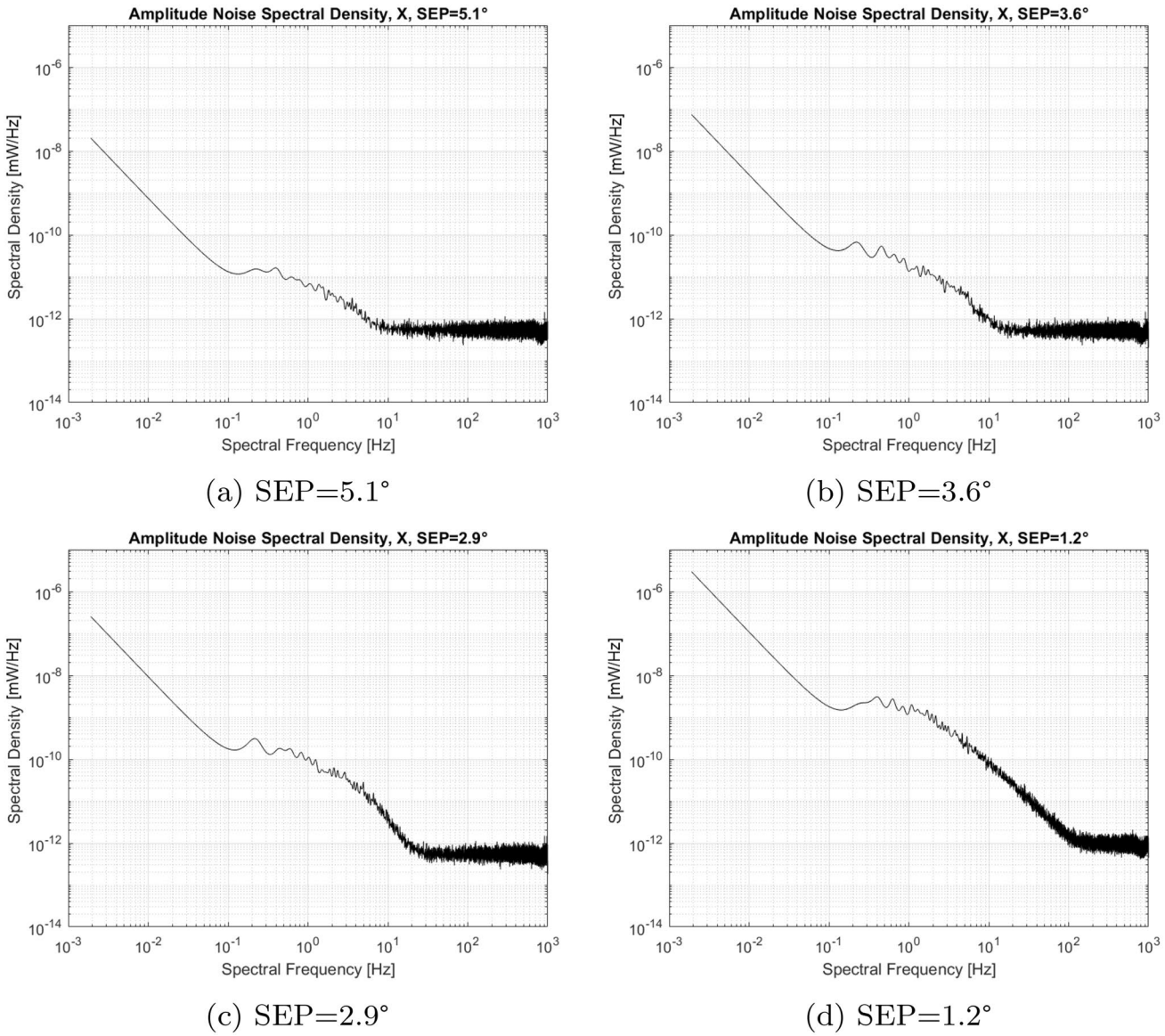

Fig. 3 Spectral density derived from the X-band measurement data. Compare the thermal noise floor for spectral frequency higher than 10 Hz with Table 1

density and to compare the amplitude scintillation index of amplitude fluctuations of the signal versus the NASA JPL model [4, 12]. The relatively good match between the JPL amplitude scintillation formulas with ESA's BepiColombo measurement data for X-band and Ka-band at small SEP angles, i.e. from 5.1° to 1.2° for the radio frequency transmission, by considering the factors 1, 1.5 and 2.41 for different solar wind activities, confirms again the suitability of these JPL amplitude scintillation formulas for the verification of the measurements for future interplanetary missions. The solar scintillation noise spectral density for X-band and Ka-band increases beyond about 0.1 Hz for increasing SEP angles. For an extremely small SEP angle of 1.2° the power spectral density will be significantly increased up to 100 Hz. On one hand these modified amplitude scintillation characteristics directly indicate the solar wind activities and can be used for future mission planning of X-band and

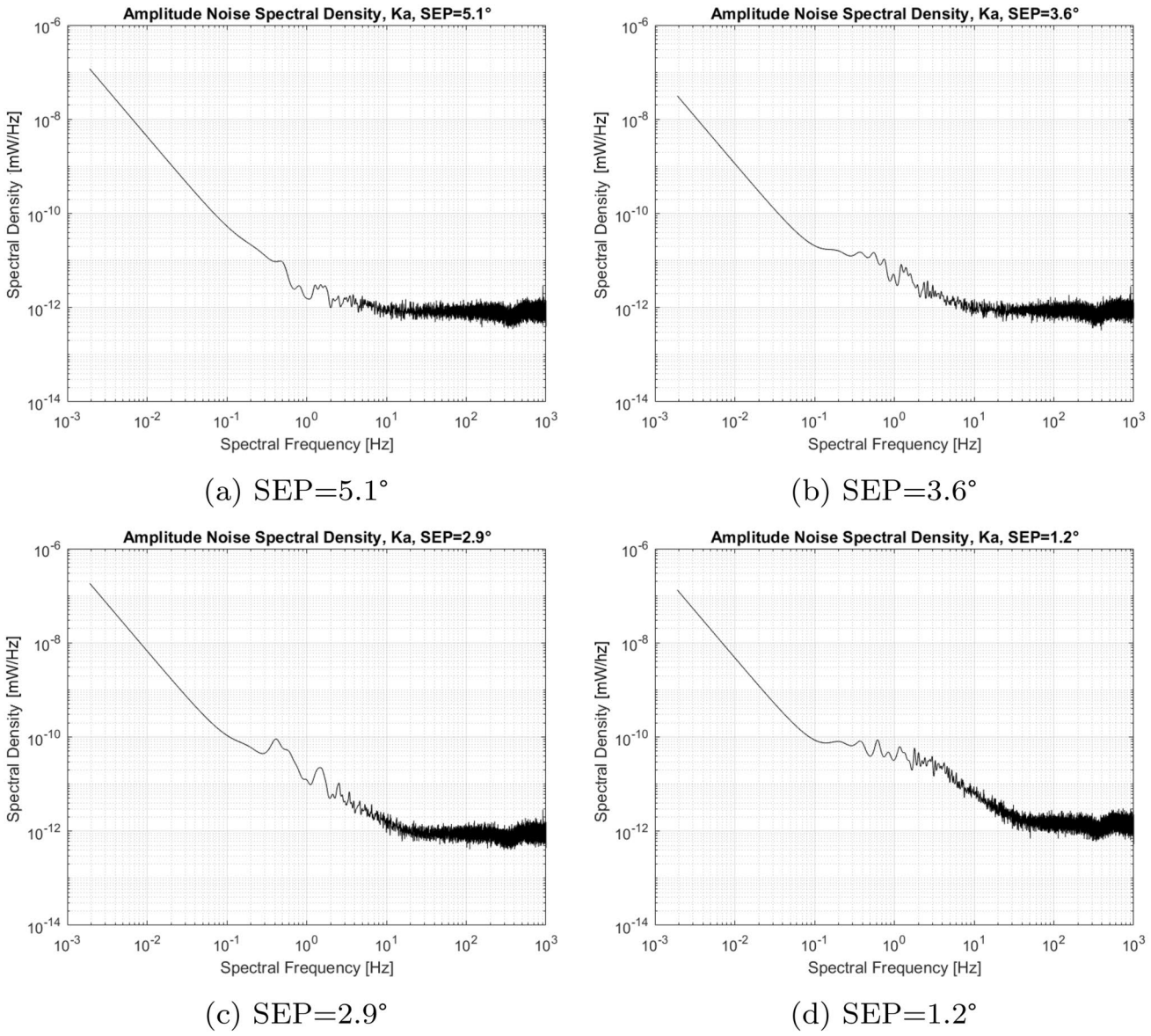

Fig. 4 Spectral density derived from the Ka-band measurement data. Compare the thermal noise floor for spectral frequency higher than 10 Hz with Table 1

Ka-band radio frequency communication links between the earth ground station and the spacecrafts. On the other hand measurement results of the amplitude and phase scintillation can be used to observe and analyze the solar coronal ejections, and to prewarn the possible strong solar wind particles propagating to Earth.

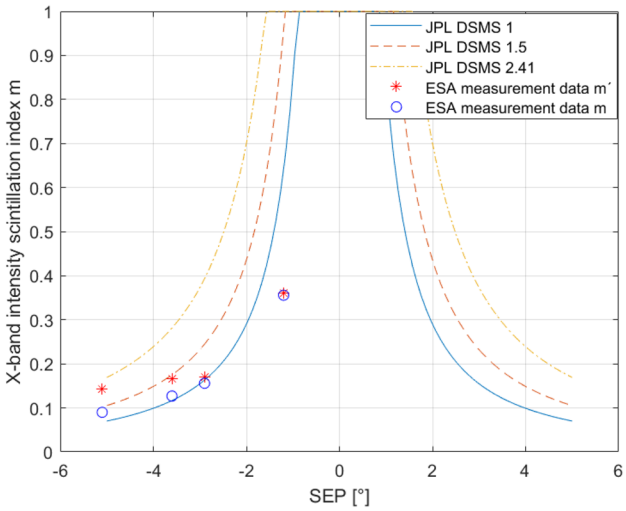

Fig. 5 Scintillation index derived from the X-band measurement data [9] depending on SEP angles

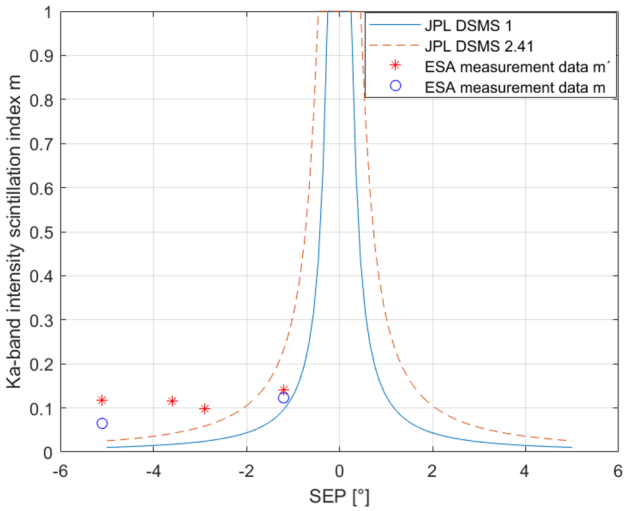

Fig. 6 Scintillation index derived from the Ka-band measurement data [9] depending on SEP angles. The m' for SEP 2.9° and SEP 3.6° are shown as sum of the solar scintillation and additive Gaussian noise which could not be removed, since the condition (4) is not valid

Acknowledgements Shun-Ping Chen would like to thank many colleagues of the Department of Electrical Engineering and Information Technologies, Institute of Communication Technologies of Darmstadt University of Applied Sciences h-da, and European Space Agency, Operations Centre ESA/ESOC for the very good cooperation. He also likes to thank his friend and colleague Prof. Dr. Heinz Schmiedel for many fruitful discussions and for carefully proofreading this paper. Finally he likes to thank the editors and the anonymous reviewers for many valuable proposals to improve the quality of this paper.

Funding Open Access funding enabled and organized by Projekt DEAL.

Declarations

Conflict of interest The authors have no relevant financial or non-financial interests to disclose. The authors have no competing interests to declare that are relevant to the content of this article. All authors certify that they have no affiliations with or involvement in any organization or entity with any financial interest or non-financial interest in the subject matter or materials discussed in this manuscript. The authors have no financial or proprietary interests in any material discussed in this article.

References

1. Woo, R.: Multifrequency techniques for studying interplanetary scintillations. Astrophys J **201**, 238–248 (1975)
2. Woo, R.: Radial dependence of solar wind properties deduced from helios 1/2 and pioneer 10/11 radio scattering observations. Astrophys J. **219**, 727–739 (1978)
3. Woo, R., Armstrong, J.W.: Spacecraft radio scattering observation of the power spectrum of electron density fluctuations in the solar wind. J Geophys Res. **84**, A12 (1979)
4. Kinman, P.W., Paal, L.: DSMS Telecommunications Link Design Handbook, 810-005, Rev. E, 34-m and 70-m Telemetry Reception. (2003)
5. David, D.: Morabito, Shervin Shambayati, Susan Finley, David Fort, The Cassini May 2000 solar conjunction. IEEE Trans Antennas Propag. 51(2). (2003)
6. David D. Morabito: "Solar Corona Amplitude Scintillation Modeling and Comparison to Measurements at X-Band and Ka-Band", IPN Progress Report. p. 42-153. (2003)
7. Lanucara, M.: Spacelink Impairments by Solar Effects. ESA/ESOC Document, Issue 2, Rev.0. (2013)
8. Chen, S.P., Villalvilla, J.: Comparison of modified Woo's solar phase scintillation model with ESA's BepiColombo superior solar conjunction measurement data for X-band and Ka-band. CEAS Space Journal, Springer Nature, New York (2022)
9. Villalvilla, J.: Selected X-band and Ka-band solar plasma measurement data of ESA BepiColombo superior solar conjunction. E-Mails on June 10, 2021 and on July 30. (2021)
10. Feria, Y., Belongie, M., McPheeters, T., Tan, H.: Solar Scintillation Effects on Telecommunication Links at Ka-Band and X-Band. TDA Progress Report. p. 42-129. (1997)
11. Ho, C.M.: DSN Telecommunications Design Handbook. 106, Rev. B, Solar Corona and Solar Wind Effects. California Institute of Technology, (2010)
12. Marco Lanucara, Rebeca Martinez-Gil, Filippo Concaro, Mattia Mercolino, Measurements of amplitude scintillation and spectral broadening in superior solar conjunction with ESA deep space probes. 4th ESA International Workshop on Tracking, Telemetry

and Command Systems for Space Applications TTC: 11–14 September 2007 at ESOC. Darmstadt, Germany (2007)
13. Matlab, https://www.mathworks.com